**The self-similar nature of natural sequences of binary scatter operations**

Scatter operators are a natural consequence of TLM. They have direction and magnitude. We work with trains of impulsive signals where the reflection operator acting on a unit magnitude pulse will cause it to move back on its track by one position and multiplies the amplitude by $\rho$. The action of the transmission operator has different definitions in one, two and three dimensions. In one-dimension an incoming pulse moves one position forward from its current position and the current magnitude is multiplied by $\tau$. In two-dimensions there is scatter in three possible directions so that

$$\rho + 3\tau = 1$$

Any further formulation requires a knowledge of the direction of the incoming pulse and in this treatment, we will consider an initial pulse arriving in from the left

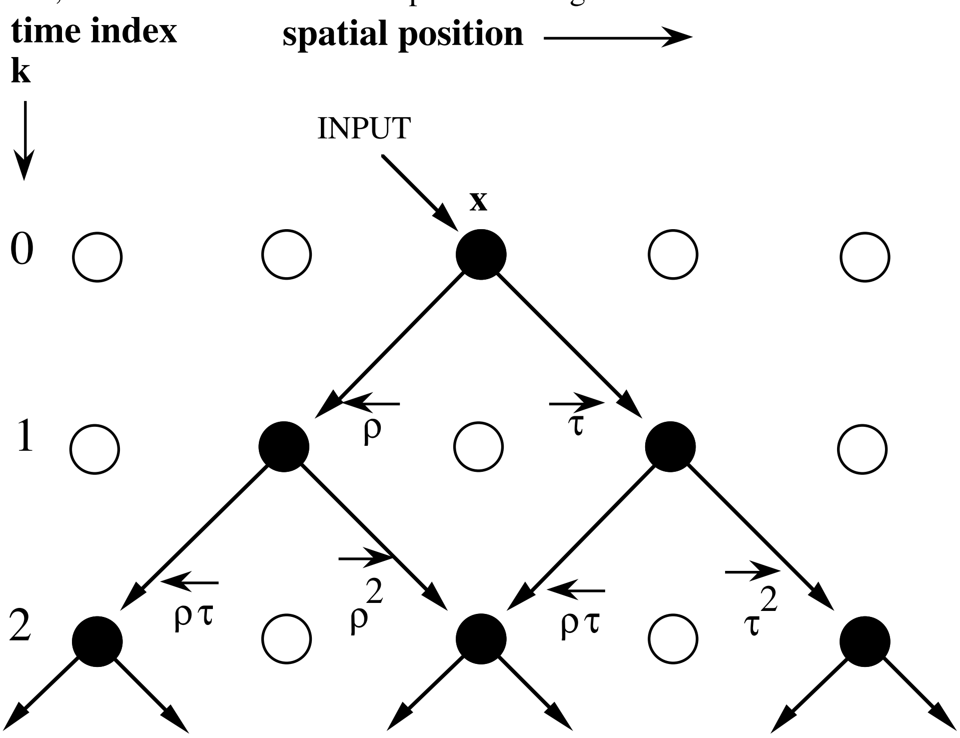


**Figure 1** Asymmetric scatter diagram for an initial input from the left

In this case we have

$$\hat{\rho}(x) = \rho(x-1) \quad \text{and} \quad \hat{\tau}(x) = \tau(x+1)$$

which is shown at level k = 1 in Figure 1

At the next scatter event we now have two pulses, one of magnitude $\rho$ moving left and one of magnitude $\tau$ moving right. These undergo binary scatter and at k = 2 we have four pulses whose position and magnitude can be determined from a set of operations which follows the natural counting sequence from least significant to most significant component.

$$\hat{\rho}\,\hat{\rho}(x) = \rho^2(x-1+1) = \rho^2(x)$$

$$\hat{\rho}\,\hat{\tau}(x) = \rho\tau(x+1-1) \;= \rho\tau(x)$$

$$\hat{\tau}\,\hat{\rho}(x) = \tau\rho(x-1-1) = \tau\rho(x-2)$$

$$\hat{\tau}\,\hat{\tau}(x) = \tau^2(x+1+1) \;= \tau^2(x+2)$$

So this and the results for k = 2 in figure 1 shows that the final positions for the naturally enumerated sequence of $2^2$ scatter operators is [0, 0, -2, 2]. We want to identify what happens after an arbitrary number of steps

Hypothetical physical processes such as single-shot injection of heat into a material can be treated as a situation where initially the input is split equally between left and right. We start with an arbitrary input of 2 units, so that one unit moves to the left and one unit moves to the right. Figure 2a shows the situation for a pulse which arrives in from the left (as described above. If this figure is reflected through its apex then we can see what happens for pulses incident from the right. The shaded region in figure 2a shows what is called 'the domain of influence'. This determines the extent of diffusion of the scatter contributions at any subsequent time. The spatial diffusion profile can then be expressed as the superposition of the domains of influence for initially left and right-going pulses. Each of these two domains is then the result of all scatter paths that start at the apex of the space-time triangle as in figure 1.

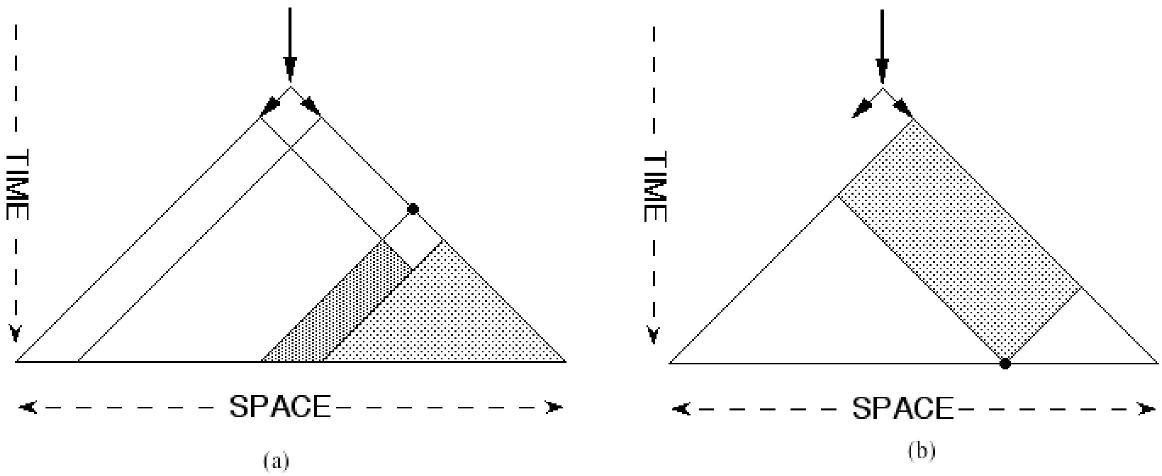


Figure 2 One-dimensional TLM scatter diagrams with initial injection share equally between left and right (a) domains of influence (shown shaded) of an individual point. (b) domain of dependence (for initially left-going pulse) of an individual point in a scatter diagram. The similar domain for the initially right-going pulse will be longer and thinner.

In figure 2b we see 'the domain of dependence' - any spatial point at an arbitrary time after injection contains only contributions from earlier scatters within the shaded region. In other words the population at any position comprises only those scatter paths that start at the apex and end at the point in question. Clearly, this is of interest as it delivers an intuitive picture of what is happening in diffusion at various levels of detail [refs to macro/micro transitions].

There are 8 components in the sequence $\hat{\rho}\hat{\rho}\hat{\rho}(x)$ to $\hat{\tau}\hat{\tau}\hat{\tau}(x)$ and their final positions can be summarised as [-1, 1, -1, 1, 1, -1, -3, 3]. There are 16 components in the sequence $\hat{\rho}\hat{\rho}\hat{\rho}\hat{\rho}(x)$ to $\hat{\tau}\hat{\tau}\hat{\tau}\hat{\tau}(x)$ and their final positions can be summarised as [0, 0, -2, 2, 0, 0, -2, 2, 0, 0, 2, -2, -4, 4]. These sequences can be plotted and the situation for $2^6$ components is shown in figure 3. A similar plot for $2^7$ components is shown in figure 4. It is quite clear that each possesses a high level of self-similarity, although the odd and even sequences are quite different

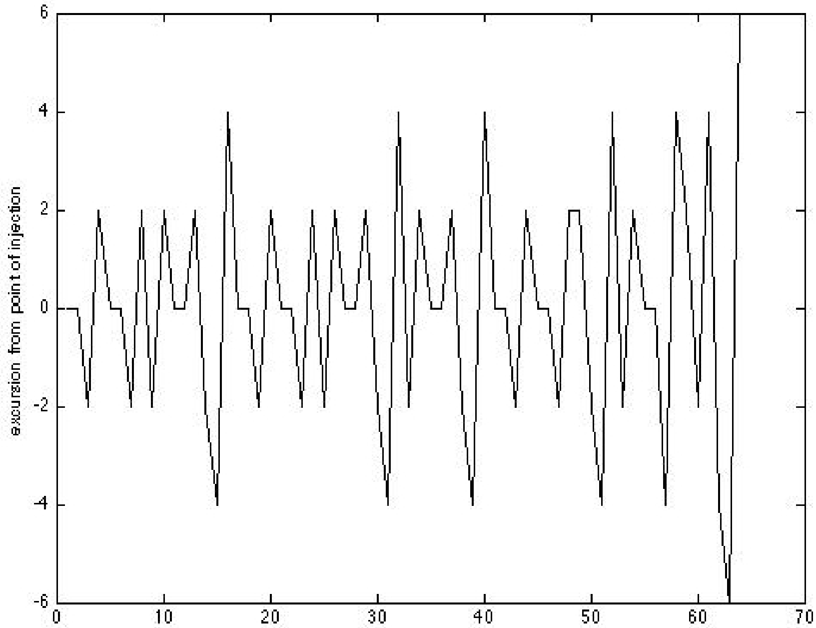


Figure 3 Excursion from the point of injection of each of the 64 components in a 6-bit (even) enumerated binary sequence

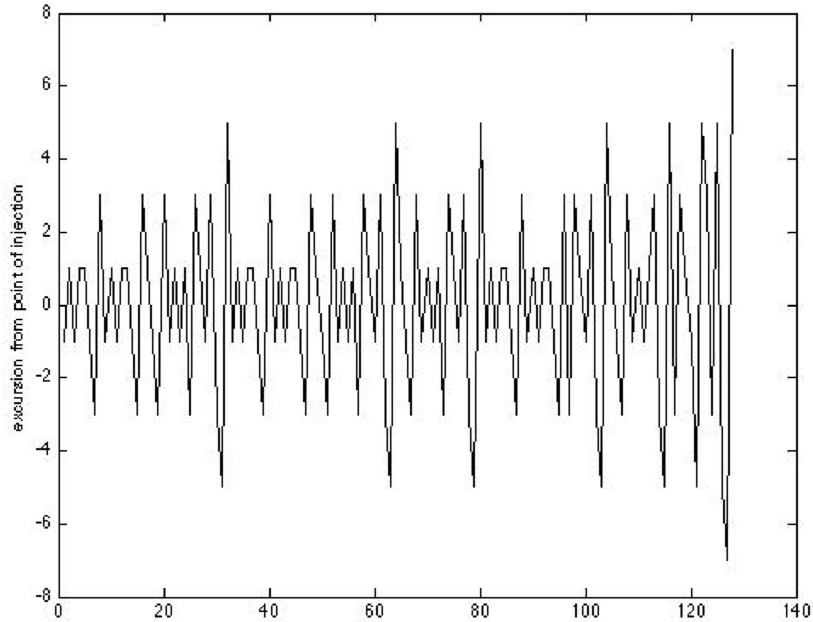


Figure 4 Excursion from the point of injection of each of the 128 components in a 7-bit (odd) enumerated binary sequence

We can gain an insight into what is happening by presenting the data for the first few sequences in a tabular format

Table I

| k | end position for each component in sequence |
|---|---|
| 0 | (0) |
| 1 | (-1, 1) |
| 2 | (0, 0),(-2, 2) |
| 3 | (-1, 1), (-1, 1), (1, -1), (-3, 3) |
| 4 | (0, 0, -2, 2), (0, 0, -2, 2), (-2, 2, 0, 0), (2, -2, -4, 4) |
| 5 | (-1, 1, -1, 1, 1, -1, -3, 3) (-1, 1, -1, 1, 1, -1, -3, 3), (1, -1, -3, 3, -1, 1, -1, 1), (-3, 3, 1, -1, 3, -3, -5, 5) |

For further discussion it would appear to be useful to separate out the odd and even sequences and only consider the situation where the initial pulse was incident from the left. Let us start with k = 2 which we can represent as

$$A_2 = (0, 0, \text{-}2, 2)$$

At k = 4 we can identify four groups of components. The first two are the same as at k = 2.

$$A_4 = A_2\ A_2\ B_2\ C_4$$

It can be seen that $B_2 = (\text{-}2, 2, 0, 0)$ and what we have designate as $C_4 = (2, \text{-}2, \text{-}4, 4)$

The same situation can be applied to k = 5

$$A_5 = A_3\ A_3\ B_3\ C_5$$

where $A_3 = (\text{-}1, 1, \text{-}1, 1, 1, \text{-}1, \text{-}3, 3)$

By this point we can also see that if we write $A_3 = (\text{-}1, 1, \text{-}1, 1), (1, \text{-}1, \text{-}3, 3) = A_3(L), A_3(R)$ then
$B_3 = A_3(R), A_3(L) = (1, \text{-}1, \text{-}3, 3), (\text{-}1, 1, \text{-}1, 1)$ There is a folding over in the middle of $A_3$.

$$C_5 = C_I, C_{II}, (-5, 5)$$

In order to define the components $C_I$ and $C_{II}$ we designate
$A_3(R) = (1, \text{-}1), (\text{-}3, 3) = A_3(R(L)), A_3(R(R))$

$C_I = (\text{-}3, 3, 1, \text{-}1, ) = A_3(R), A_3(L)$ i.e. the folding of $A_3(R)$

$C_I = (3, \text{-}3\ )$ i.e. the folding of $A_3(R(R))$

So, for any naturally enumerated sequence with $2^n$ components we can write the final positions as
$$A_n = A_{n-2}\ A_{n-2}\ B_{n-2}\ C_n$$

$$A_{n-2} = A_{n-4} A_{n-4} B_{n-4} C_{n-2} = A_{n-2}(L), A_{n-2}(R)$$

$$B_{n-2} = B_{n-4} C_{n-2} A_{n-4} A_{n-4} = A_{n-2}(R), A_{n-2}(L)$$

$$C_n = C_I \; C_{II} \; C_{III} \cdots C_{N-(n-1)} \; (-n, n)$$

The sequence $A_{n-2}(R)$ can be split as $A_{n-2}(R(L)), A_{n-2}(R(R))$

$$C_I = A_{n-2}(R(R)), A_{n-2}(R(L))$$

The sequence $A_{n-2}(R(R))$ can be split as $A_{n-2}(R(R(L))), A_{n-2}(R(R(R)))$

$$C_{II} = A_{n-2}(R(R(R))), A_{n-2}(R(R(L)))$$

This process is repeated for (n-1) folds until we have

$$C_{N-(n-1)} = (-(n-1), (n-1))$$

**Other properties of natural sequences of binary scatter operators.**
A conventional phase plot ($Y_{n+1}$ vs $Y_n$) appears quite confused, even for small systems.

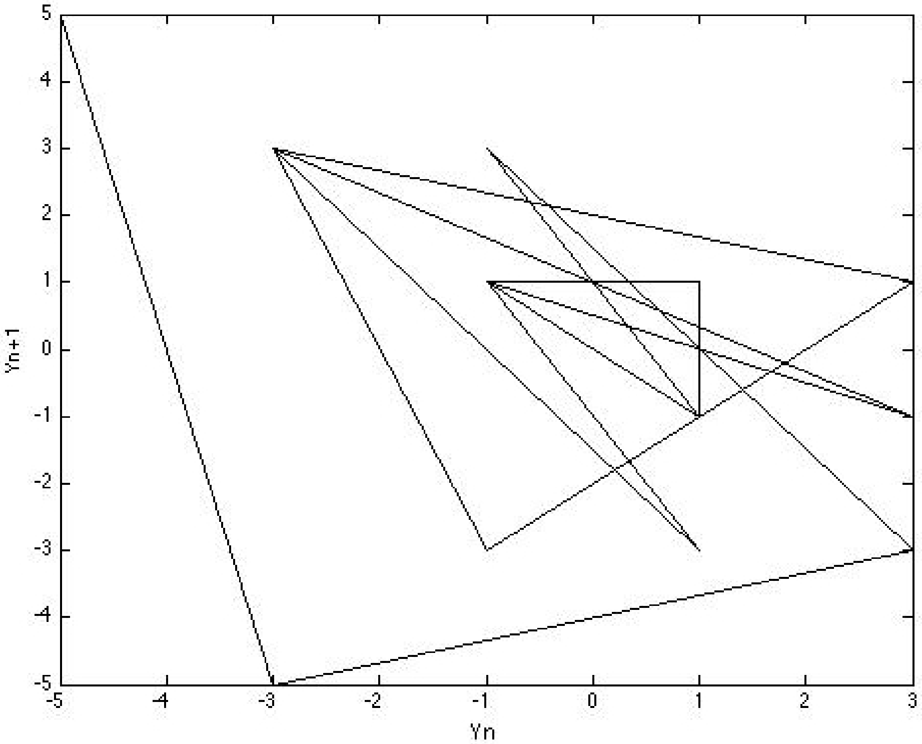


Figure 5(a) A plot of $Y_{n+1}$ against $Y_n$ where $Y_n$ and $Y_{n+1}$ are sequential excursions from the point of injection in a 5-bit enumerated binary scatter sequence

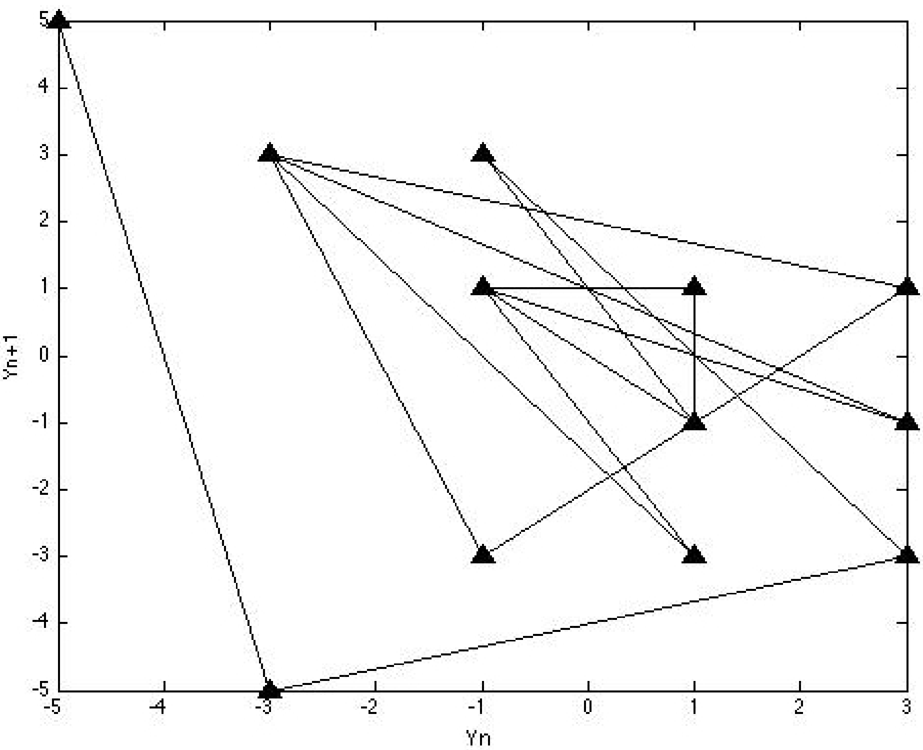


Figure 5(b) As per figure 5(a) with markers showing the points of excursion.

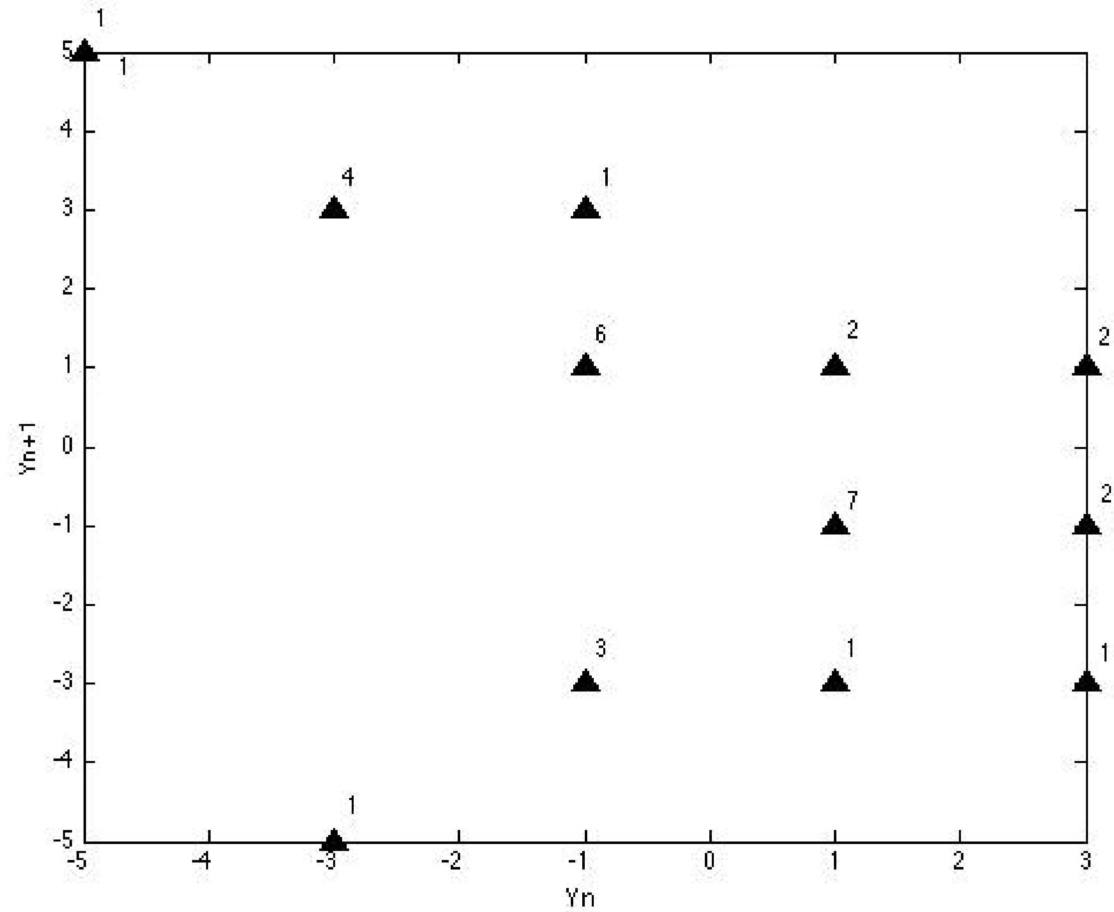


Figure 5(c) As per figure 5(b) with connecting lines removed. The numbers next to the triangles show the frequency of occurrence of each of the points. This is summarised in the table below

| $Y_n$ | $Y_{n+1}$ | Frequency |
|---|---|---|
| -5 | 5 | 1 |
| -3 | -5 | 1 |
| -3 | 3 | 4 |
| -1 | -3 | 3 |
| -1 | 1 | 6 |
| -1 | 3 | 1 |
| 1 | -3 | 1 |
| 1 | -1 | 7 |
| 1 | 1 | 2 |
| 3 | -3 | 1 |
| 3 | -1 | 2 |
| 3 | 1 | 2 |

The results for a much larger odd bit sequence are shown below. All appear to have the same character: two arms extending above and below the vertical axis for all $Y_n < 0$ and a solid triangle of occupied points for all $Y_n > 0$.

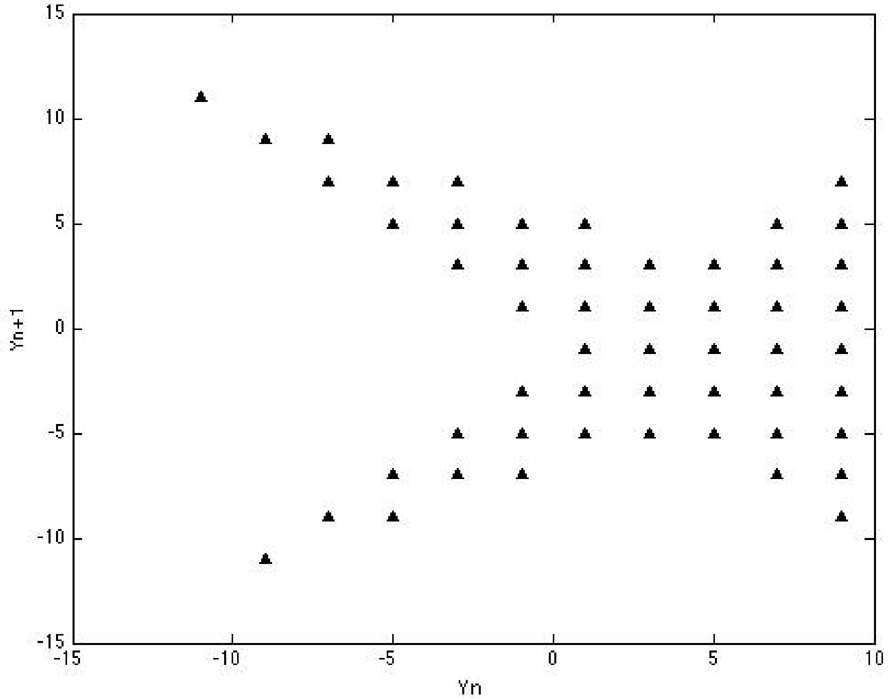


Figure 6 A plot of $Y_{n+1}$ vs $Y_n$ for a eleven-bit enumerated binary scatter sequence

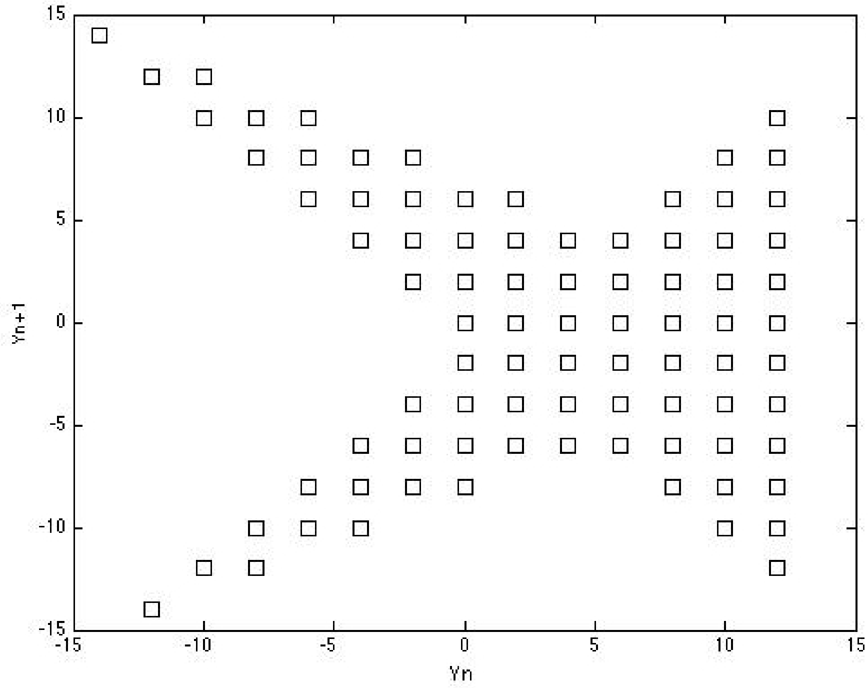


Figure 7 A plot of $Y_{n+1}$ vs $Y_n$ for a fourteen-bit enumerated binary scatter sequence

When the first 2048 points of figure 7 are superimposed on the data in figure 6 we see how the odd and even bit sequences are interlaced (figure 8)

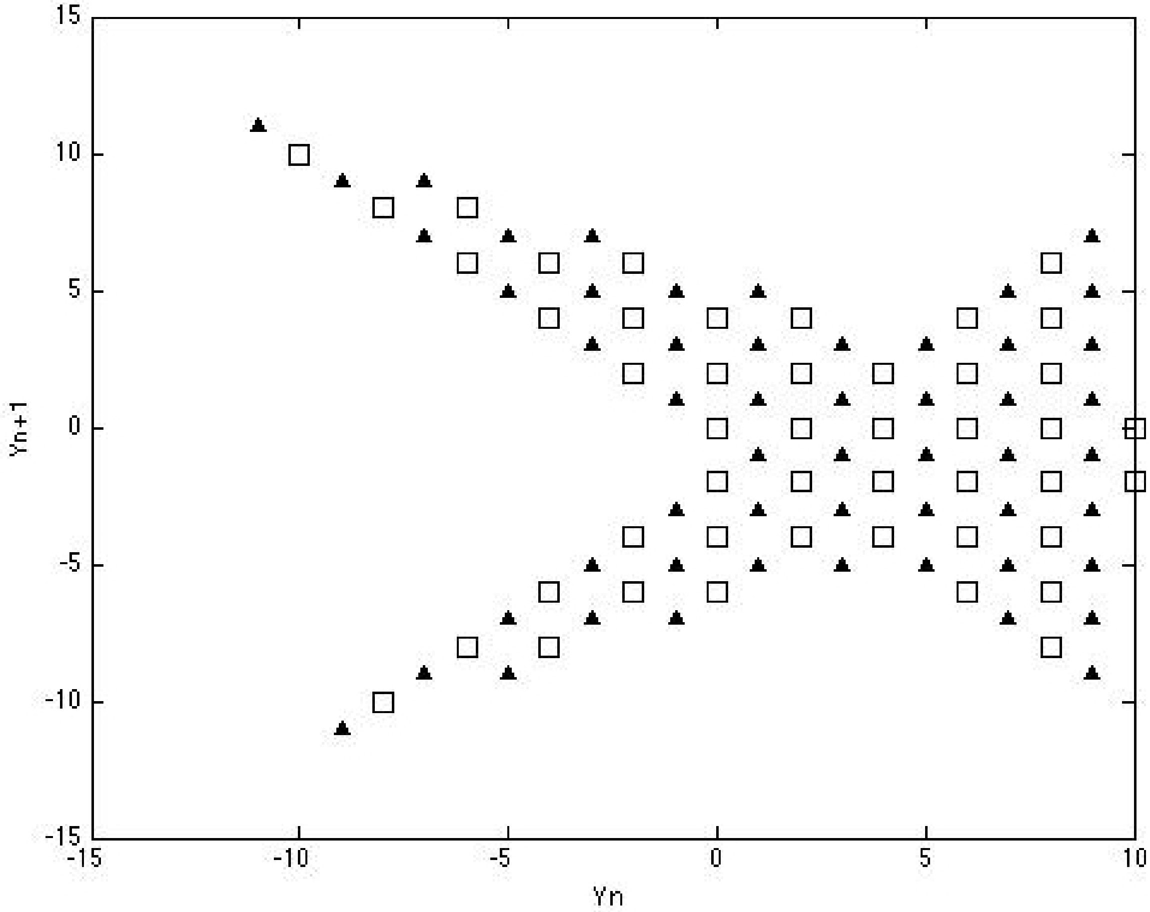


Figure 8 $Y_{n+1}$ vs $Y_n$ for odd (triangles) and even (squares)-bit enumerated binary scatter sequence

**The frequency spectrum of enumerated binary scattering**

The cyclic nature of components such as (-1,1), (1,-1) etc suggests that there should be a discernable Fourier spectrum and as the data is always radix 2 an FFT should be appropriate. FFTs have been undertaken for odd and even sequences and it has been found that for reasonable sample sizes (greater than 1024 data points), the character and the relative amplitude does not change. Thus a 10 bit and a 12 bit sequence have indistinguishable character (and similarly for odd sequences). It was noted that there was some difference between even and odd sequences and this has been compared by taking normalised frequency vs normalised amplitude for both cases. Results are shown in Figure 9(a) and (b) below

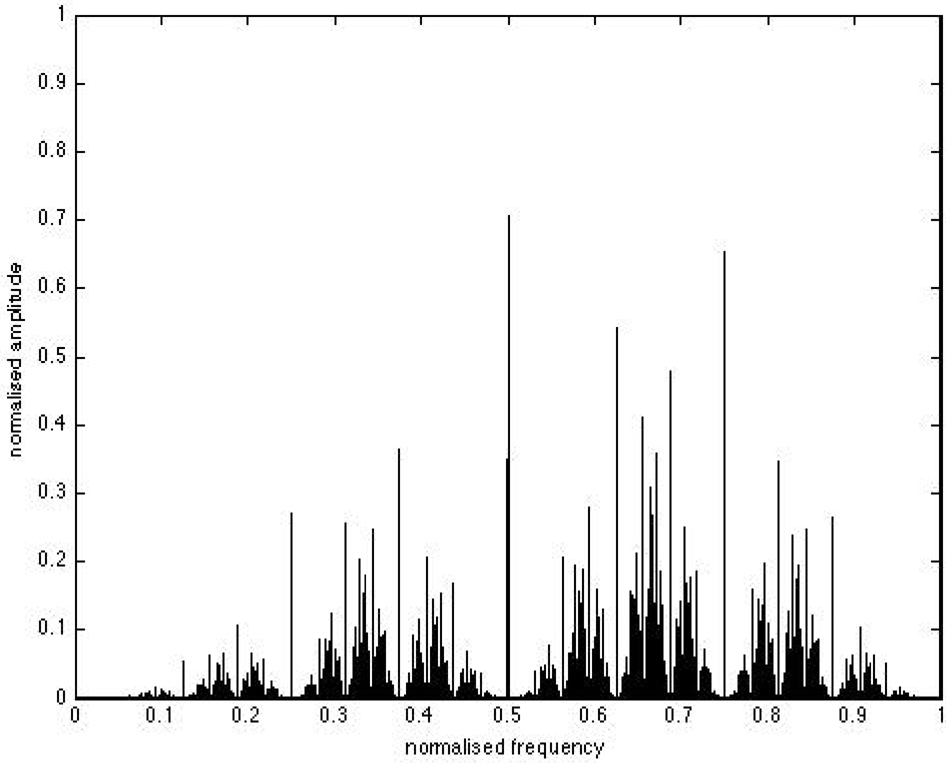


Figure 9(a) Normalised frequency vs normalised amplitude for an 21-bit sequence

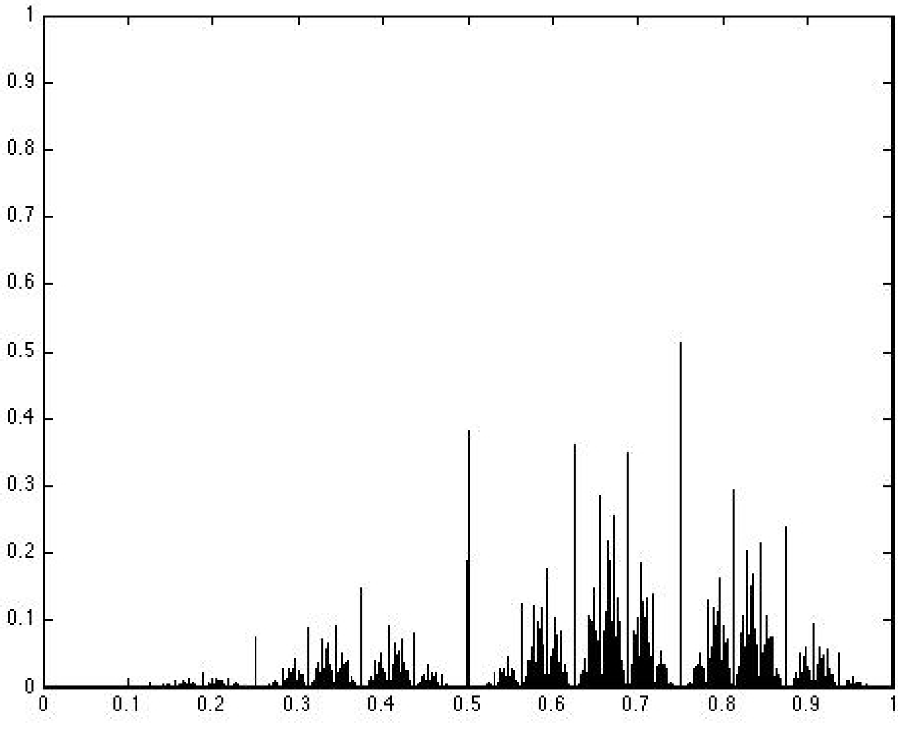


Figure 9(b) Normalised frequency vs normalised amplitude for an 20-bit sequence